Towards reproducible, scalable lateral molecular electronic devices

Colm Durkan[1,*] & Qian Zhang

[1]: Nanoscience Centre, University of Cambridge, 9 JJ Thomson Avenue, Cambridge CB3 0FA, United Kingdom

*: email: cd229@eng.cam.ac.uk

(Dated: May 2014)

An approach to reproducibly fabricate molecular electronic devices is presented. Lateral nanometer-scale gaps with high yield are formed in Au/Pd nanowires by a combination of electromigration and Joule-heating-induced thermomechanical stress. The resulting nanogap devices are used to measure the electrical properties of small numbers of two different molecular species with different end-groups, namely 1,4-butane dithiol and 1,5-diamino-2-methylpentane. Fluctuations in the current reveal that in the case of the dithiol molecule devices, individual molecules conduct intermittently, with the fluctuations becoming more pronounced at larger biases.

PACS numbers:

Keywords:

Molecular electronics has undergone somewhat of a renaissance in recent years, due in part to the fact that silicon-based devices have continued to decrease in size towards molecular dimensions. Transistors have been fabricated with gate lengths as short as 3 nm [1], and a plethora of new architectures have been either proposed or demonstrated where devices can be grown in a bottom-up fashion using nanowires [2, 3], wrapped-gates [4, 5] and various other modalities [6, 7]. Of course, the cost of making such devices combined with their reduced efficiency and yield is somewhat of a bottleneck in terms of mass-production, and at present, it appears as if this is a fundamental rather than technical issue [8]. Therein lies the renewed interest in molecular systems. The underlying principles are that molecules are to be used as the central current-controlling entity within a device, and as molecules of a particular species can be synthesised to all be identical, issues related to reproducible fabrication should become irrelevant. Unfortunately, while this may be the case for the molecules themselves, the same cannot be said for the contacts to those molecules. A number of different methodologies have been employed to achieve reliable contact to molecules, including Scanning Tunneling Microscopy (STM) [9, 10], mechanically-controlled break junctions (MCBJs) [11-14] and vertical cross-wire sandwich junctions [15-17]. Atomic switches have been demonstrated whereby a voltage applied across a cross-wire device can reversibly and reproducibly create an atomic bridge [18, 19]. However, the first two of these approaches, whilst capable of measuring electrical transport through single molecules with unprecedented precision and control, suffer from not being scalable. Sandwich junctions on the other hand tend to suffer from pinholes and unintentional, irreversible short-circuits. For this reason, in this article, we present results from lateral devices that are scalable in principle.

The work presented here builds on earlier reports of a simple and reproducible process based on electromigration and Joule heating that can be used to create nanometer-scale gaps in Au/Pd nanowires [20]. An alternative approach whereby a feedback loop is used to control the electromigration process has been reported [21, 22], but as yet, there are no reports involving the application of these nanogaps to the field of molecular electronics. The overall process concept is as follows. Step 1: Gold/Palladium nanowires are fabricated by electron-beam lithography with length 1 μm, thickness 35 nm and width in the range 40-80 nm (Supplementary information, Figure 1). They are fabricated on 44 nm of thermally-grown SiO_2 on Si. Step 2: these nanowires are failed using electromigration combined with thermomechanical stress, and

subsequently tested for stable tunnelling characteristics. Step 3: molecules are inserted from solution. Step 4: the devices are tested. As reported earlier, Au/Pd is chosen as the nanowire material for two reasons: (i) the mean grain size is typically 5-8 nm, meaning that even wires as narrow as the ones we fabricate have a polycrystalline rather than bamboo microstructure, (ii) Au is suitable for molecular attachment to molecules with thiol or amine end groups. The microstructure is important, as the failure point for bamboo-type wires is less well-controlled than for polycrystalline wires. The smaller grains lead to larger resistance as compared to Au nanowires, and an as-fabricated wire typically has a 4-terminal resistance of the order 500 Ω. This is irrelevant given that the resistance of the molecular devices/junctions is at least several MΩ as we will see later. The devices are failed by a combination of electromigration and thermomechanical stress, by applying a voltage ramp at the rate 3 mV s^{-1}. When the voltage across the wires is in the range 1.3-1.4 V, the power being dissipated in the wires reaches around 1 mW, and they reach a peak temperature of approximately 250^{o} C from Joule heating and they fail towards the anode end (an indication that electromigration alone is not leading to failure) with nanometer-scale gaps. 80% of the gaps formed in this way display tunnelling with a gap size of 2 nm or less as determined from a fit of the tunnelling current to the Simmons-type model for tunnelling in the intermediate voltage range ($eV < \varphi$), where e is the electron charge [23-25]. Given that the gaps are so small, the form of $J(V)$ including the image potential is used. This is accurate for gap sizes about around 1.5 nm, but the solution to Simmons' model diverges for smaller gaps and an alternative approach should be taken thereafter [26]. In Fig. 1(a), we show the distribution in gap sizes obtained by performing least-squares fits to Equation 50 from reference 23 on post-failure tunnelling curves such as those shown in Fig. 1(b). A number of alternative failure modes are observed during our experiments, albeit with low probability: (i) the wires catastrophically fail and the entire wire is obliterated – this happens in the event of uncontrolled spikes in voltage output from the sourcemeter, or as a result of incorrect grounding of the devices; (ii) the wires fail with a large (> 50 nm) gap at the centre of the wire, due to excessive Joule heating or if the voltage ramp rate is > 5 mV s^{-1}; (iii) the wires fail at the cathode end due to very little Joule heating and more prominent electromigration. These three modes of failure lead to the resulting tunnel current being either too small to measure or unstable and noisy, and either way, such devices are unsuitable for further use. Of the devices that do form "clean" nanogaps that display clear and stable tunnelling characteristics, the vast majority can be

successfully used for molecular transport measurements. The overall geometry of the failure zone is that the wires are tapered vertically, as shown in Fig. 1(c). This is due to the fact that electromigration proceeds most slowly along the bottom surface of a nanowire, as it is clamped to the surface, and is fastest on the three other surfaces. This means that the actual lateral extent of the effective nanogaps is considerably smaller than the cross-section of the wires, so the number of molecules that can bridge the nanogaps will tend to be small, especially if the molecules are short. This uncertainty in the exact configuration of the nanogaps leads to an error in the estimation of the gap sizes. This is not all that significant, as the molecules chosen tend to be able to bridge the nanogaps, and the variation in tunnelling characteristics between as-failed devices is not particularly large. At 1 V, the measured currents are in the range 8-22 nA, corresponding to a conductance of the order 8-22 nS, comparable to reports in the literature [27] for similar sized devices.

Once candidate devices have been identified on the chip, the entire chip is immersed in a weak (0.1 mM) solution of the molecules of interest and left overnight. The chip is then removed from solution and rinsed to remove any unbound molecules. Two molecular systems were investigated, (i) 1,5-diamino-2-methylPentane (Fig. 2(a)) and (ii) 1,4-butane dithiol (Fig. 3(a)). These are different in two ways: (i) the first molecule is around 0.7 nm long, is non-symmetric and the amine end group will form a weak bond with the gold atoms; (ii) the second molecule is around 0.97 nm long, is symmetric and the thiol end group will form a strong covalent bond with the gold atoms in the nanogap, with a number of possible binding sites [28]. In general, amine-linked molecules are considered to be preferable to thiol-linked molecules for molecular transport applications as they exhibit less localisation of electrons in the bond [28], so are more conductive. The weaker bond can however lead to instabilities in the molecule-metal junction. In single-molecule experiments, the asymmetric molecule shows asymmetric current-voltage characteristics, whereas the symmetric molecule shows symmetric characteristics. In the devices presented here, there will be more than one molecule taking part in the conduction process at any one time, so we expect symmetric characteristics irrespective of the molecule. If one desires to create a realistic (i.e. with more than one molecule) molecular device with asymmetric characteristics, then the asymmetry must be built in to the device itself.

In Fig. 2(b) and (c), we show the characteristics for the amine-linked molecular devices. There is a significant increase in conductivity after insertion of the molecules, depending on the

number of molecules bridging the gap. Results from two different devices are presented: in Fig. 2(b), we show the current-voltage characteristics from a device under both polarities of applied bias, and in Fig. 2(c), we show a different device under repeated voltage ramps (positive), where the level of reproducibility is clear. We have found that the characteristics of single devices are very stable over time, but that there is a significant spread in conductivity between devices, with a variation ranging from a 20- to 5000-fold increase in conductivity after insertion of molecules. In Fig 2(c), we show how the device characteristics vary with temperature in the narrow temperature range from 300 K to 380 K, from which it can be seen that there is a significant effect of temperature, indicative of hopping conduction. To estimate the number of molecules bridging the gap, it is known that the conductance of a similar molecule -- 1,5 diamino Pentane, at a bias voltage of 25 mV is around $3x10^{-4}$ G_0, where G_0 is the conductance quantum [29]. Our current-voltage characteristics reveal a conductance for a device of $2.6x10^{-3}$ G_0 when the voltage is 25 mV. Assuming that the conductance is not significantly modified by the presence of the additional methyl group, we can then to first order determine that the number of molecules is given by the ratio of the conductance of the device to that of a single molecule, from which we find that the number of molecules is approximately 8. In a number of cases, asymmetric current-voltage characteristics are observed (Supplementary information, Figure 2.), indicating that (i) the number of molecules is small enough that there is a difference between the number of molecules that have the methyl group closest to the left electrode and those that have it closest to the right electrode, and (ii) the current-voltage characteristics of individual molecules are indeed asymmetric. We have not observed significant asymmetries in the current-voltage characteristics for the symmetric molecules we have investigated.

In Fig 3(b) & (c), we show the results for the thiol-linked molecular devices. Here, there is a more modest 20-fold increase in conductivity after insertion of molecules. By contrast, with these molecules, we find that there is little variation between devices, of the order a factor of 2, but that there are significant fluctuations in conductivity of each device over time. From the extremes that the current switches between, it is evident that the fluctuations are by multiples of a discrete quantity, which we are ascribing to individual molecular channels switching on and off. This is not unlike random telegraph noise in its presentation, but is not necessarily due to any quantum fluctuations, and is rather more likely to be due to some molecules forming intermittent contact with the nanogap electrodes. The noise characteristics of metal-molecule-

metal junctions have been reported, and fluctuations were shown to demonstrate the presence of localised charge traps [30]. However, in that case, the current tended to fluctuate between relatively stable levels associated with trapping and detrapping, whereas our observations are over a range of levels, indicative of a different mechanism. The ratio of the total current to the minimum fluctuation size we observe was 10 for one device and 16 for the other, indicating that for one device, an average of 10 molecules formed contacts with the gold electrodes, whereas it was 16 molecules for the other device. This is comparable to the number of molecules we expect to be present in the amine-linked devices. Using wires with smaller cross-section (predominantly the width) will allow even smaller numbers of molecules to be probed. It can also be seen from Fig. 3 that the fluctuations in current become larger as the bias voltage is increased, indicating that such a device is not suitable for use above a bias voltage of around 1 V.

To conclude, we have presented a scheme for testing the electrical properties of small numbers of molecules ($< \sim 20$) that is reliable, inherently reproducible and ultimately scaleable. Multiple independent devices can be fabricated on a single substrate, and in principle can be tested in parallel. We have used this scheme to measure the transport characteristics of two different molecules – 1,4 butane dithiol and 1,5 diamino 2-methyl pentane. We found that the thiol-terminated molecular devices displayed erratic jumps in conductivity, which we ascribed to individual molecules forming intermittent contact with the electrodes. The amine-terminated molecules displayed significantly larger conductivity, albeit with a larger spread in characteristics.

The author would like to acknowledge the assistance of two project students who assisted with the measurements, Qian Zhang and Min Li.

REFERENCES

1. Hyunjin Lee et al, 2006 Symposium on VLSI Technology, 58, 2006, DOI: 10.1109/VLSIT.2006.1705215
2. K. Tomioka, M. Yoshimura & T. Fukui, *Nature*, **488**, 189 (2012)
3. G. Larrieu & X. –L. Han, *Nanoscale*, **5**, 2437 (2013)
4. A. D. Franklin, S. O. Koswatta, D. B. Farmer, J. T. Smith, L. Gignac, C. M. Breslin, S. J. Han, G. S. Tulevski, H. Miyazoe, W. Haensch & J. Tersoff, *Nanoletters*, **13**, 2490 (2013)
5. E. Leobandung, J. Gu, L. Guo & S. Y. Chou, J. Vac. Sci. Technol. B **15**, 2791 (1997)
6. H. M. Yamamoto, M. Nakano, M. Suda, Y. Iwasa, M. Kawasaki & R. Kato, *Nature Communications*, **4**, 3379 (2013)
7. J. Shi, S. D. Ha, F. Schoofs & S. Ramanathan, *Nature Communications*, **4**, 2676 (2013)
8. M. J. Kelly, *Nanotechnology*, **22**, 245303 (2011)
9. F. Moresco & A. Gourdon, *PNAS*, **102**, 8809 (2005)
10. X. D. Cui et al, *Science*, **294**, 571 (2001)
11. B. Xu & N. J. Tao, *Science*, **301**, 1221 (2003)
12. M. A. Reed, C. Zhou, C. J. Muller, T. P. Burgin & J. M. Tour, *Science*, **278**, 252 (1997)
13. J. He, O. Sankey, M. Lee, N. Tao, X. Li & S. Lindsay, *Faraday Discuss.*, **131**, 205 (2006)
14. H. Vazquez, R. Skouta, S. Schneebeli, M. Kamenetska, R. Breslow, L. Venkataraman & M. S. Hybertson, *Nature Nanotechnology*, **7**, 663 (2012)
15. H. Haick & D. Cahen, *Progress in Surface Science*, **83**, 217 (2008)
16. F. Chen, J. Hihath, Z. Huang, X. Li & N. J. Tao, *Annu. Rev. Phys. Chem.*, **58**, 535 (2007)
17. Y. Chen, G. –Y. Jung, D. A. A. Ohlberg, X. Li, D. R. Stewart, J. O. Jeppesen, K. A. Nielsen, J. Fraser Stoddart & R. Stanley Williams, *Nanotechnology*, **14**, 462 (2003)
18. C. Schirm, M. Matt, F. Pauly, J. C. Cuevas, P. Nielaba & E. Scheer, *Nature Nanotechnology*, **8**, 645 (2013)
19. M. Feuchsle et al, *Nature Nanotechnology*, **7**, 242 (2012)
20. F. Hadeed & C. Durkan, *Applied Physics Letters*, **91**, 123120 (2007)
21. D. R. Strachan, D. E. Smith, D. E. Johnston, T. –H. Park, M. J. Therein, D. A. Bonnell & A. T. Johnson, *Appl. Phys. Lett.*, **86**, 043109 (2005)

22. A. A. Houck, J. Labaziewicz, E. K. Chan, J. A. Folk & I. L. Chuang, *Nanoletters*, **5**, 1685 (2005)

23. J. G. Simmons, *J. Appl. Phys.*, **34**, 1793 (1963)

24. R. Stratton, *J. Phys. Chem. Solids*, **23**, 1177 (1962)

25. K. H. Gundlach, *J. Appl. Phys.* **44**, 5005 (1973)

26. A. Vilan, *J. Phys. Chem.*, **111**, 4431 (2007)

27. S. Ghosh, H. Halimun, A. K. Mahapatro, J. Choi, S. Lodha & D. Janes, *Appl. Phys. Lett.*, **87**, 233509 (2005)

28. B. Xu, N. J. Tao, *Science*, **301**, 1221 (2001)

29. L. Venkataraman, J. E. Klare, I. W. Tam, C. Nuckolls, M. S. Hybertsen & M. L. Steigerwald, *Nanoletters*, **6**, 458 (2006)

30. Y. Kim, H. Song, D. Kim, T. Lee & H. Jeong, *ACS Nano*, **4**, 4426 (2010)

FIGURE CAPTIONS

Fig. 1. **(a)** Histogram of nanogap size as extracted from Simmons' model [Ref 23], showing that the spread of gap sizes is centred on 1-2 nm; **(b)** Tunnelling current from two different as-failed, clean devices; **(c)** AFM image of as-failed nanogap, showing the tapered shape of the electrodes.

Fig. 2. **(a)** Molecular structure of 1,5 diamino 2-methyl pentane; **(b)** Current-Voltage characteristic of nanogap bridged with 1,5 diamino 2-methyl pentane molecules, **(c)** Repeated Current-Voltage measurements (positive bias ramp applied, time is on the x-axis) for 1,5 diamino 2-methyl pentane molecules showing reproducibility of current transport; **(d)** Temperature dependence of the current through a device, showing a significant increase in current with increasing temperature, indicative of hopping conduction.

Fig. 3. (a) Molecular structure of 1,4 butane dithiol; **(b)** & **(c)** Current-voltage characteristics of two different devices bridged with 1,4 butane dithiol molecules. In both cases, the current before and after molecular insertion is shown.

(a)

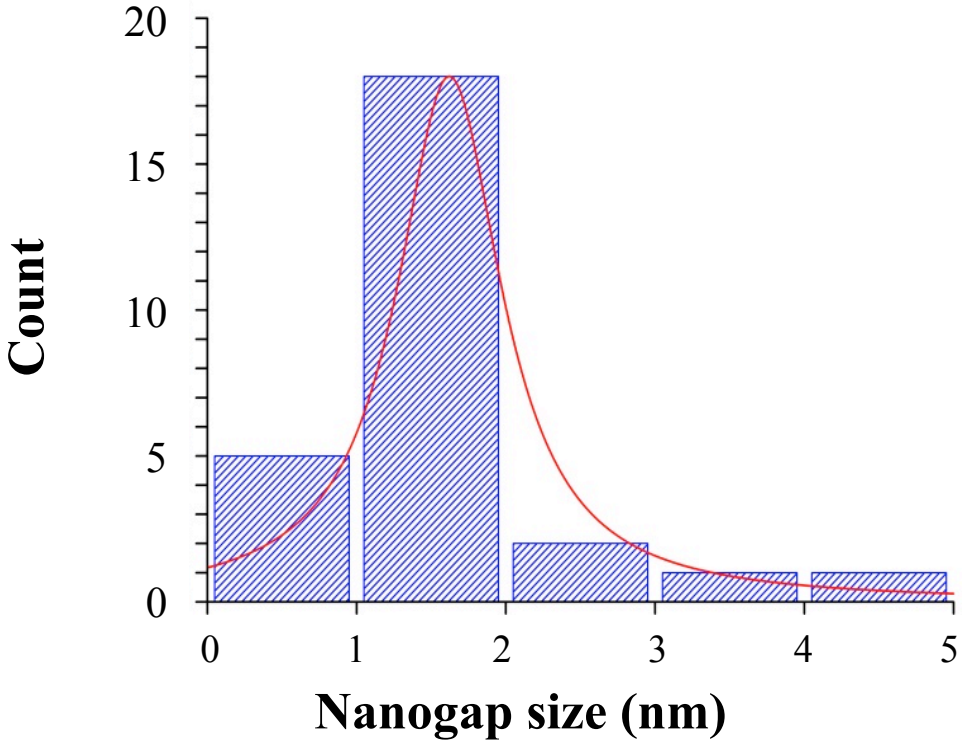
Count
20
15
10
5
0
0
1
2
3
4
5
Nanogap size (nm)

(b)

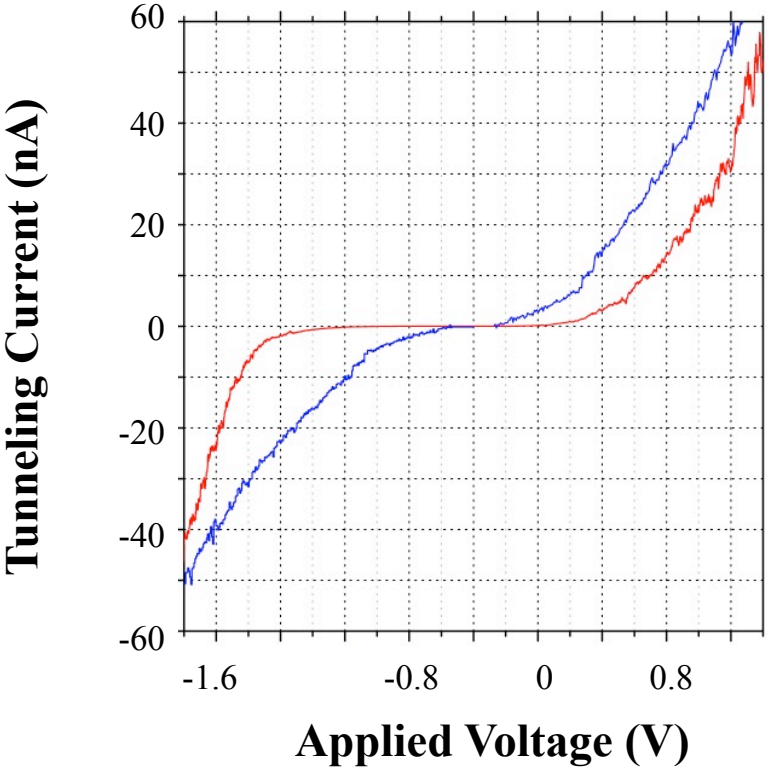
Tunneling Current (nA)
60
40
20
0
-20
-40
-60
-1.6
-0.8
0
0.8
Applied Voltage (V)

(c)

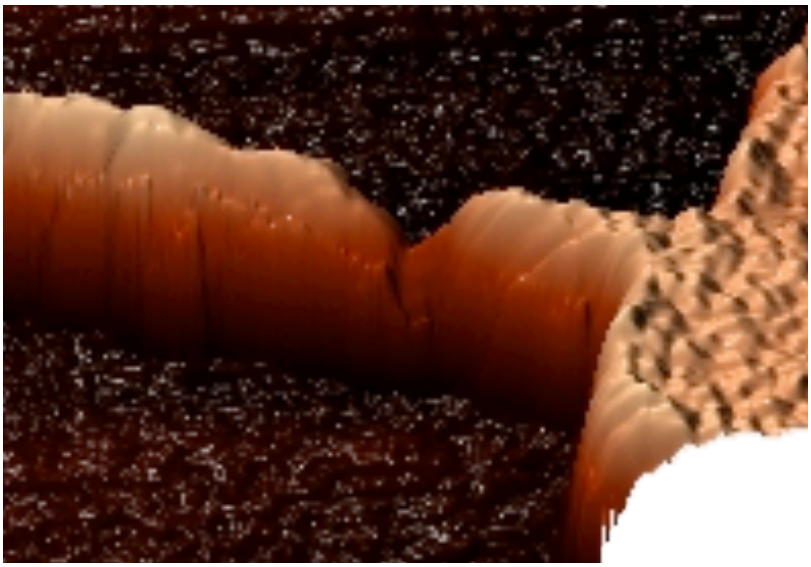

Fig. 1 DURKAN

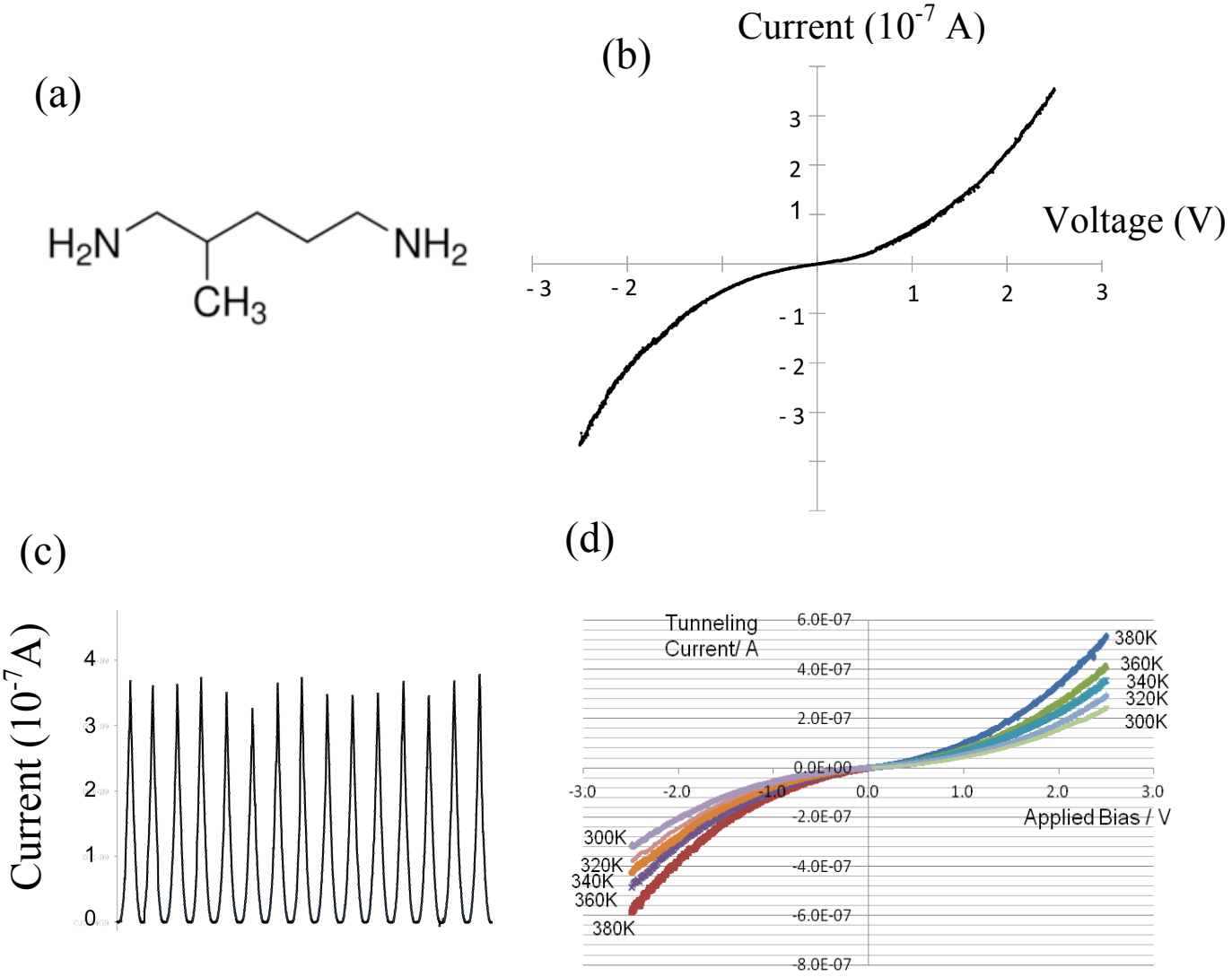
(a)
H2N
NH2
CH3
(b)
Current (10-7 A)
Voltage (V)
3
2
1
- 3
- 2
1
2
3
- 1
- 2
- 3
(c)
Current (10-7A)
4
3
2
1
0
(d)
Tunneling Current/ A
6.0E-07
4.0E-07
2.0E-07
0.0E+00
-2.0E-07
-4.0E-07
-6.0E-07
-8.0E-07
-3.0
-2.0
-1.0
0.0
1.0
2.0
3.0
Applied Bias / V
380K
360K
340K
320K
300K
300K
320K
340K
360K
380K

Fig. 2. DURKAN

(a)

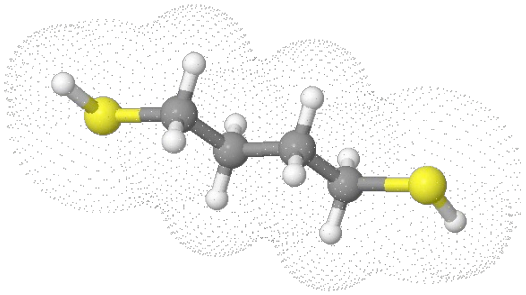

(b)

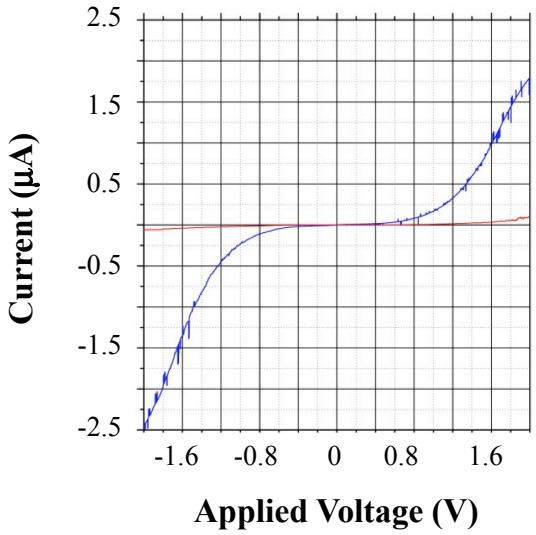

(c)

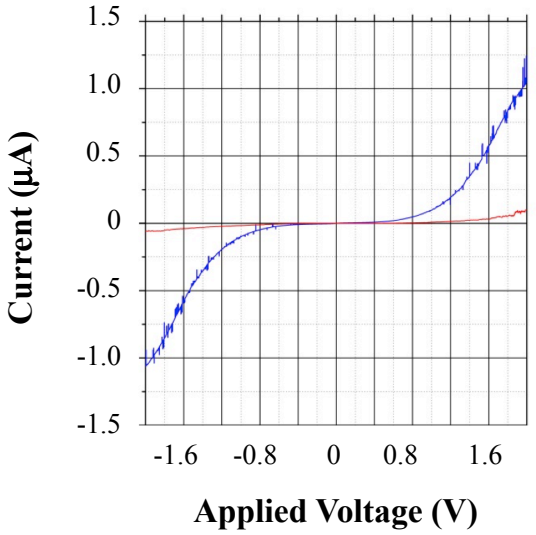

Fig 3. DURKAN